

Structural phase transformations and the equations of state of calcium chalcogenides at high pressure

Huan Luo, Raymond G. Greene, Kouros Ghandehari, Ting Li, and Arthur L. Ruoff

Department of Materials Science and Engineering, Cornell University, Ithaca, New York 14853

(Received 27 June 1994)

The crystal structures of three calcium chalcogenides CaS, CaSe, and CaTe were investigated by energy-dispersive x-ray-diffraction techniques using a synchrotron source to a static compression up to 52 GPa. For CaS and CaSe, a first-order phase transformation from the NaCl phase to the CsCl phase was observed at 40 and 38 GPa, respectively. For CaTe, it first transforms from the NaCl phase to an intermediate state possibly with a mixture of NaCl and MnP phases at 25 GPa, and then to the CsCl phase above 33 GPa. The phase transitions were reversible with small hysteresis. The equations of state and bulk moduli were obtained for all three compounds. The systematic behavior among the calcium chalcogenides under compression and the unusual transition sequence of CaTe are discussed.

I. INTRODUCTION

The combination of modern diamond-anvil cell techniques and the use of synchrotron sources for x-ray diffraction has provided unique opportunities for high-quality crystalline structural investigation of solids at pressures up to multimegabars. High-pressure experimental research on structural phase transformations has been approaching a stage of systematic study and understanding of a series of materials with analogous physical and/or chemical properties. An example can be found in the III-V semiconducting compounds, where the structural, optical, and electrical properties at high pressure have been extensively studied.¹ The pressure-induced structural phase transition and insulator-metal transition are also of great theoretical interest since they provide good tests for theoretical predications.

The alkaline-earth chalcogenides (AX : $A = \text{Be, Mg, Ca, Sr, Ba}$; $X = \text{O, S, Se, Te}$) form a very important closed-shell ionic system crystallized in the NaCl-type ($B1$) structure at ambient conditions except for the MgTe and the beryllium chalcogenides. A feature in the electronic band structure of the AX compounds is that there are no d electrons in the valence band. The band gaps in the AX compounds range from about 2.5 to 6 eV. Under compression, a first-order phase transition from the sixfold-coordinated $B1$ structure to the eightfold-coordinated CsCl-type ($B2$) structure has been found in all barium and strontium chalcogenides with only one exception found in BaO. BaO was reported to experience two intermediate phases before approaching the $B2$ phase.²⁻⁴ The light and middle AX compounds ($A = \text{Be, Mg, Ca}$) have not been systematically investigated. Among the calcium chalcogenides, CaO is known to have the $B1$ - $B2$ transition at 61 GPa,⁵ and the $B2$ phase is stable to at least 135 GPa.^{6,7} CaTe has been studied by a conventional x-ray-diffraction method with an unidentified intermediate phase reported at about 32 GPa and the $B2$ phase at 35 GPa.⁸ Logically, one would expect a similar transition sequence ($B1$ - $B2$) for the rest of the calcium chalcogenides, i.e., CaS and CaSe, with tran-

sition pressures between that of CaTe and CaO. It was our hope to verify this and to identify the intermediate phase in CaTe.

This paper presents the experimental results of high-pressure energy-dispersive x-ray-diffraction (EDXD) measurements on CaX ($X = \text{S, Se, Te}$) and the data analysis which leads to determinations of the high-pressure crystal structure and equations of state for these three compounds. This work is a part of our global investigation on the structural and electronic properties of the III-V and II-VI compounds under static compression.

II. EXPERIMENTAL TECHNIQUES

The EDXD experiments on CaX were performed at the Cornell High Energy Synchrotron Source (CHESS). Details of the EDXD experiments are given in Refs. 9 and 10. CaS (99.99% purity), CaSe (99.5% purity), and CaTe (99.5% purity), all in a form of fine powder, were each loaded in a diamond-anvil cell (DAC) along with gold powder which served as an internal pressure marker. The pressure in the sample was determined by the isothermal equation of state of gold obtained from the shock-wave method.¹¹ The diamond-anvil flats and the sample hole sizes used in the experiments were 450 and 150 μm in diameter, respectively. In these experiments we first used a tungsten-rhenium (W/Re) alloy (75% W and 25% Re) as gasket in the DAC because the alloy, while maintaining very high strength, is not as brittle as either pure tungsten or pure rhenium. The performance of W/Re gaskets was quite satisfactory with less sample hole shape changes radially than that of the steel gaskets at a given pressure. To avoid decomposition of these hygroscopic ionic salts, no pressure medium was used. The x-ray beam passed through a $20\ \mu\text{m} \times 20\ \mu\text{m}$ aperture before striking the sample. The data were collected at a diffraction angle $\theta \approx 7.15^\circ$ (its accurate value was determined by the diffraction data from the internal gold marker at 1 atm).

For all three samples, the ambient condition x-ray-diffraction spectra have the $B1$ structure diffraction

features, including peak intensities. The measured lattice constants of all three compounds at 1 atm are in good agreement with literature values. The results on CaTe were repeated because of its complicated structural behavior seen in the first run. The highest pressure attempted on these samples was 52.1 GPa and all measurements were taken at room temperature.

III. RESULTS

A. Calcium sulfide

The lattice constant of CaS at 1 atm measured by this work is $a_0 = 5.689$ Å. The *B1* phase of CaS is stable with increasing pressure until 39.6 GPa, at which the relative volume V/V_0 is 0.727. A diffraction spectrum at this pressure is shown in Fig. 1(a). Starting at 39.9 GPa, a structural phase transition starts with a new peak that represents a new phase clearly seen at 22.70 keV [see Fig. 1(b)]. The new phase and the *B1* phase coexist with further increasing pressure for about 5 GPa before the transformation is completed at about 45 GPa. Above 45 GPa, the diffraction patterns can be fully indexed to the *B2* structure with good interplanar distance (d spacing) and intensity agreements between the observed and calculated values. The sample in the *B2* phase was further

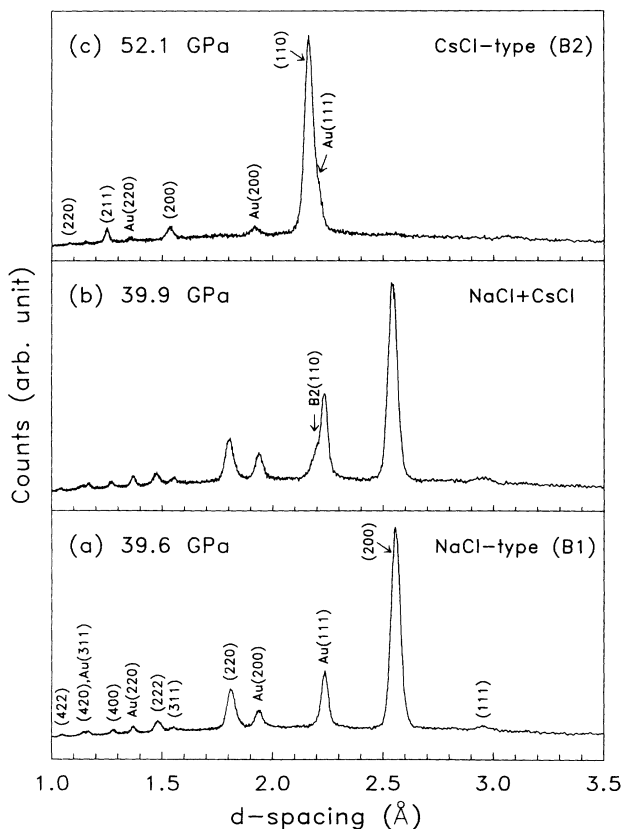


FIG. 1. EDXD spectra of CaS around the *B1*-*B2* transition. The x-ray energy has been converted to d spacing as shown in the x axis. Those labeled by Au are diffraction peaks from the gold marker. Those unlabeled peaks in (b) are the same as the corresponding peaks in (a).

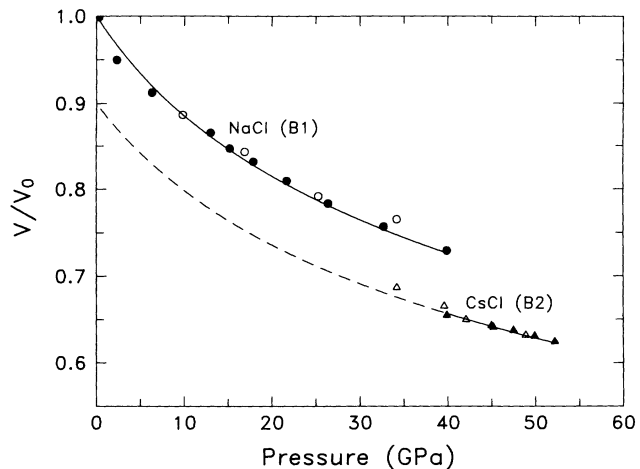


FIG. 2. Plot of the relative volume V/V_0 of CaS versus pressure. The solid lines are the Birch fits. The decompressing data are shown by open symbols and are not used in data fitting.

compressed to 52.1 GPa with no phase transition observed. A diffraction spectrum of the fully transformed sample at 52.1 GPa is shown in Fig. 1(c).

Upon decreasing pressure from 52.1 GPa, a completely reverse process was recorded with the *B2*-*B1* transition first observed at 34.2 GPa. Thus, the equilibrium *B1*-*B2* transformation pressure (the average value of the compressing and decompressing transition pressures) in CaS is determined to be 37.1 ± 2.9 GPa.

At the first coexistence of the *B1* and *B2* phases in CaS, the atomic volumes (the unit-cell volume divided by the number of atoms per unit cell) are 16.739 and 15.024 Å³ in the *B1* and *B2* phase, respectively. Therefore, the decrease in relative atomic volume on transformation is $-\Delta V/V(B1) = 10.2\%$. At 52.1 GPa, the *B2* structure has an atomic volume of 14.314 Å³, corresponding to a volume reduction of 0.622, the largest compression reached.

The P - V relation of CaS is plotted in Fig. 2, along with a fit to the two parameter Birch equation¹²

$$P = \frac{3}{2}B_0(x^{7/3} - x^{5/3})[1 + \frac{3}{4}(B_0 - 4)(x^{2/3} - 1)], \quad (1)$$

where $x = V_0/V$, B_0 is the isothermal bulk modulus at zero pressure, and B'_0 is the first-order pressure derivative of the bulk modulus evaluated at zero pressure. Both *B1* and *B2* phases have nearly the same values of B_0 and B'_0 determined at 64 GPa and 4.2, respectively. The extrapolated relative volume of the *B2* phase at zero pressure is $V_0(B2)/V_0(B1) = 0.90$.

B. Calcium selenide

The lattice constant of CaSe at 1 atm measured in this work is 5.916 Å. CaSe undergoes the same structural transition sequence as that of CaS described above. The *B1*-*B2* transition in CaSe starts at 37.5 during uploading with a relative volume decrease of 7.7%. This transformation is not completed until 42 GPa. Three selected diffraction spectra around the *B1*-*B2* transition are

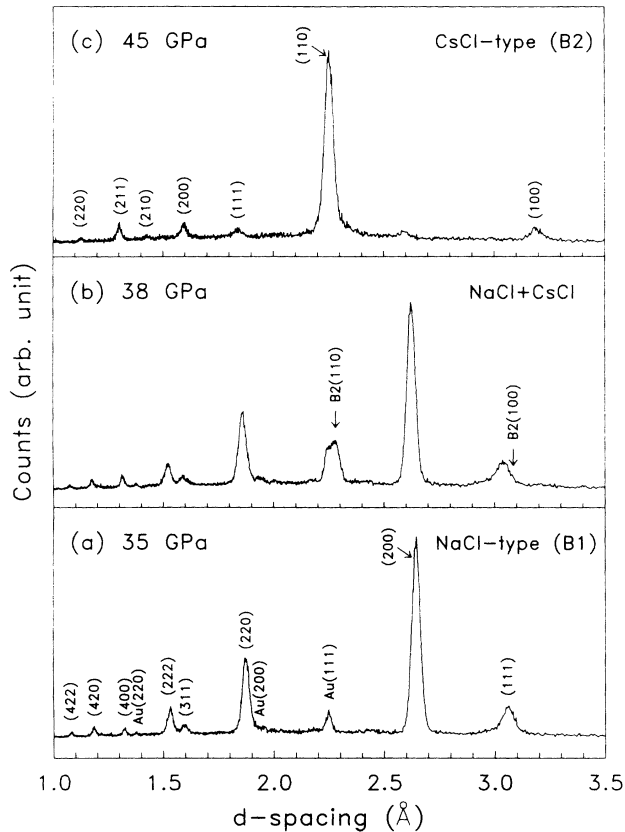


FIG. 3. EDXD spectra of CaSe around the $B1$ - $B2$ transition. The x-ray energy has been converted to d spacing as shown in the x axis. Those labeled by Au are diffraction peaks from the gold marker. Those unlabeled peaks in (b) are the same as the corresponding peaks in (a).

shown in Fig. 3. The uploading process is fully reversible during decompression with the $B2$ - $B1$ transformation first observed at 30.2 GPa. Thus, the equilibrium transition pressure in CaSe is 33.9 ± 3.7 GPa.

The P - V relation is plotted in Fig. 4 with the Birch fit

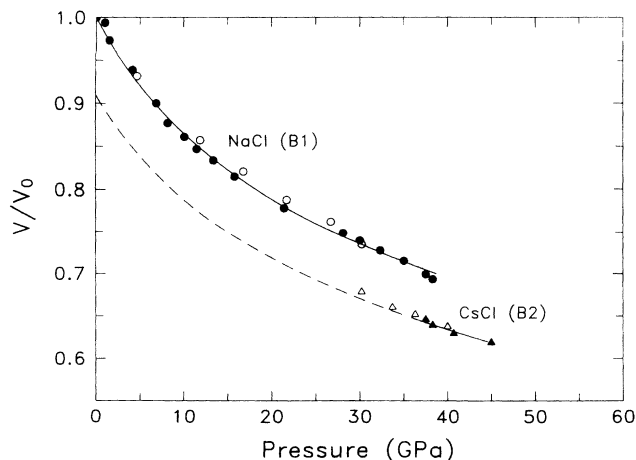


FIG. 4. Plot of the relative volume V/V_0 of CaSe versus pressure. The solid lines are the Birch fits. The decompressing data are shown by open symbols and are not used in data fitting.

[Eq. (1)] shown in solid lines. The Birch parameters are $B_0 \approx 51$ GPa and $B'_0 \approx 4.2$ for both $B1$ and $B2$ phases. The extrapolated relative volume of the $B2$ phase at zero pressure is 0.91.

C. Calcium telluride

Three typical diffraction spectra of CaTe are shown in Fig. 5. The x-ray-diffraction pattern of CaTe at 1 atm [Fig. 5(a)] measured from the DAC can be indexed to the $B1$ structure with satisfactory d spacing and intensity fits. The measured lattice constant is $a_0 = 6.348$ Å. However, in comparison to the $B1$ phase diffraction spectra of CaS and CaSe, the low-pressure diffraction spectra of CaTe contain two very weak peaks in the region of 15–25 keV which can not be indexed to the face-centered-cubic (fcc) $B1$ structure. One will see later that these peaks grow with increasing pressure and initialize a new structure. It seems that a small fraction of the sample is in a non- $B1$ phase. This is likely because the ratio of cation and anion radii in CaTe is quite large ($r_c/r_a = 2.23$), approaching the critical value for the ionic solids ($r_c/r_a = 2.41$) with the $B1$ structure.

The $B1$ phase in CaTe could be followed with increasing pressure up to about 23 GPa. At 22.2 GPa, the rela-

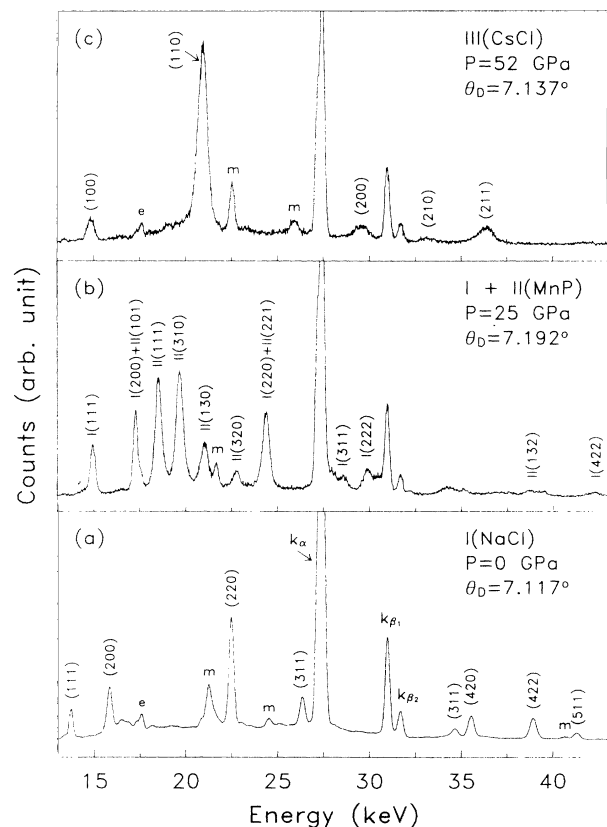


FIG. 5. EDXD spectra of CaTe at three selected pressures. The pressure, phase assignment, and diffraction angle for each spectrum are shown in the upper right corners. The tellurium fluorescence peaks are indicated by k_α and k_β . Those labeled by symbols e and m represent escape peaks from the Ge detector and the diffraction peaks from the gold marker, respectively.

tive volume is 0.752. Starting at 24.7 GPa, there was a dramatic change in diffraction spectra indicated by several new intense peaks in the region of 18–22 keV. Figure 5(b) shows a typical spectrum in this region. The new peaks cannot be indexed to the *B1* structure. The *B1* phase could still be indexed at and above 24.7 GPa but with an incorrect intensity relation between the peak at 17.28 keV if assigned as *B1*(200) and the peak at 24.38 keV if assigned as *B1*(220). It should be noted that the new peaks had started at lower pressures and only became significant above 24 GPa.

The next task is to index the diffraction spectra above 24 GPa. We note that the *B1* structure has a sixfold coordination. According to the general trend of pressure-induced structural phase transformation, one would look for a structure with either six- or eightfold coordination. So far, the binary compounds with the *B1* structure have been reported to transform to, in addition to the most common *B2* structure, the NiAs,^{2–4} the body-centered-tetragonal [HgTe and HgSe (Refs. 13–15)], and the orthorhombic structures (PbX, X=S, Se, Te).¹⁶ In the case of CaTe, we have failed to fit our spectra above 24 GPa to several hexagonal and tetragonal structures, including the NiAs, PH₄I, β -Sn, and body-centered-tetragonal structures. We have also examined the distorted *B1* structures with the bases unchanged and the simple cubic arrangement, but without success. The failure came either from poor *d* spacing fits or unreasonable atomic volumes which must be less than that in the *B1* phase at lower pressures.

The most reasonable fit of *d* spacing for the diffraction lines other than that of the *B1* structure came from an indexing to an orthorhombic unit cell with parameters $a = 8.061$ Å, $b = 7.362$ Å, and $c = 3.076$ Å at 24.7 GPa. Regarding the basis in the unit cell, the following constraints were applied for the structural (basis) determination. (1) Reasonable atomic volume compared to that in the *B1* phase at the same pressure; (2) reasonable diffraction intensity agreement between observed and calculated values; (3) coordination number which should be six or higher; (4) reasonable nearest-neighbor distances which cannot be less than a certain value; (5) the shape of unit cell that should be similar to the structure to be assigned. Under these requirements, we propose a two phase mixture of the NaCl phase and the MnP phase for the pressure region 25–31 GPa. The indexings of the two phase region are shown in Fig. 5(b).

The MnP structure contains four ion pairs per unit cell generally at $\pm(u\nu\frac{1}{4}; \frac{1}{2}-u, \nu+\frac{1}{2}, \frac{1}{4})$ and belongs to the space group *Pbnm*. Here, *u* and *ν* are adjustable parameters, depending on each compound with this structure. The MnP structure can be described as a distortion of that of the NiAs structure¹⁷ and has been assigned to the intermediate phase in FeS at high pressure.¹⁸ Our fitted values for *u* and *ν* are $u(\text{Te}) = 0.527$, $\nu(\text{Te}) = 0.346$; and $u(\text{Ca}) = 0.646$, $\nu(\text{Ca}) = 0.031$. With these values, the number of nearest neighbors (coordination number) for both Te and Ca ions is approximately six at distances ranging from 2.49 Å (Ca-Te) to 3.07 Å (Ca-Ca or Te-Te). For comparison, at the same pressure the shortest Ca-Te distance in the *B1* structure is 2.87 Å. At 24.7 GPa, the

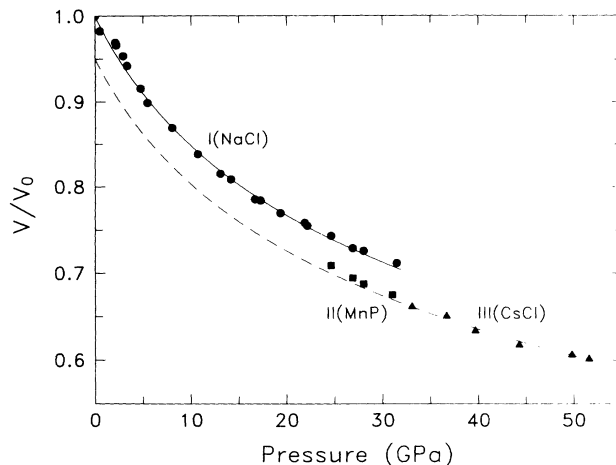


FIG. 6. Plot of the relative volume V/V_0 of CaTe versus pressure. Data from different phases are shown with different symbols. The solid lines are the Birch fits.

atomic volume is 23.68 Å^3 for the *B1* phase and 22.76 Å^3 for the MnP phase, corresponding to a 4% volume decrease.

With further increase of pressure, a second phase transformation started at about 33 GPa. Above 33 GPa, the diffraction spectra can be fully indexed to the *B2* structure. Both *d* spacing and intensity agree well with the calculated values. There is no significant volume discontinuity at this transformation. Figure 5(c) shows a fully transformed diffraction spectrum of CaTe at 52 GPa. Two calculated peaks (111) and (220) based on the *B2* structure with relative intensities of 11.6 and 10.0 %, respectively, were not observed, indicating an existence of texturing.

As pressure was released from 52 GPa, the *B2* phase started to transform to an intermediate phase at about 29 GPa. The decompressing diffraction data were insufficient in quality to support any structural determination in this intermediate phase, although they showed some feature(s) of the MnP-type diffraction pattern; and the *B1* phase was not present at this pressure. The *B1* phase was not observed until further decrease of the pressure to about 22 GPa. The transformation to the *B1* phase was completed at about 1 GPa.

Figure 6 shows a plot of relative volume versus pressure along with a Birch fit [Eq. (1)] to the data points. The Birch fit gives $B_0 \approx 41.8$ GPa and $B'_0 \approx 4.3$ for both *B1* and *B2* phases. Because of lack of data points in the intermediate phase between 25–33 GPa, we did not fit the data points in this region.

IV. DISCUSSION

Table I summarizes some important experimental results for CaX. With the current results, the structural transformations to the eightfold-coordinated *B2* structure have been achieved for all calcium chalcogenides with systematic trends scaled with the ionic radii and the lattice constants. We fitted our results and obtained the

TABLE I. Summary of major experimental results for calcium chalcogenides. Symbols used in this table have been defined in the text.

Compound	P_t (GPa)	V_t/V_0 (B1)	$-\Delta V/V_0$ (B1)	B_0 (GPa)	B'_0	Ref.
CaO	61	0.74	10%	111	4.2	7
CaS	40	0.73	10.2%	64	4.2	This work
CaSe	38	0.70	7.7%	51	4.2	This work
CaTe	33	0.74 ^a	4.6% ^a	42	4.3	This work

^aValues at the transformation to the intermediate phase.

following relations:

$$\log_{10}(P_t) = 1.056 + 1.029(r_c/r_a) \quad (2)$$

$$\log_{10}(B_0) = 0.906 + 1.620(r_c/r_a), \quad (3)$$

where P_t is the transition pressure to the $B2$ phase on loading, B_0 is the bulk modulus of the $B1$ phase, and r_c/r_a is the ionic ratio of cation-anion radii.¹⁹ The deviations in the above fitting are small. Similar empirical relations have been found in strontium chalcogenides.^{20,21}

The high-pressure eightfold-coordinated $B2$ structure in CaX is expected to be stable for a large pressure range. According to a simple model calculation²² and experimental results on cesium halides,^{23–27} ionic solids initially in the $B2$ phase could transform to a tetragonal phase at high pressure at a fractional volume of around 0.5. If this is also true for the ionic solids in the high-pressure $B2$ phase, then the instability of the $B2$ phase in CaTe , the one expected to have the lowest transition pressure among CaX , will occur in the neighborhood of 130 GPa, using our equation of state. The high-pressure $B2$ structure of ionic solids may transform into an eight-atom-based orthorhombic structure by further compression. Evidence has been found recently in alkali hydrides²⁸ for such behavior. So far, none of the alkaline-earth chalcogenides has been compressed high enough to destabilize the $B2$ structure.

We have visually examined the samples under a microscope at their largest compression of about 50 GPa and seen light transmitted through the sample. Only CaTe appeared red in color, corresponding to an absorption edge of about 2 eV. Thus, all the calcium chalcogenides are still insulators.

The relative volume decreases at the first phase transformation are 10–14 % for the entire heavy alkaline-earth chalcogenides except for CaSe ($-\Delta V/V = \sim 8\%$) and CaTe ($-\Delta V/V = \sim 4\%$). The substantial small volume collapse at transformation in CaSe and CaTe is attributed to the large disparity in their ionic radii. CaSe and CaTe have the largest ratios of ionic radii among the heavy alkaline-earth chalcogenides. The repulsive force between large ions (anions) in CaSe and CaTe resists volume collapse at transition.

The unusual phase transition sequence in CaTe may also be linked to its large ionic ratio ($r_a/r_c = 2.23$). This ratio is close to the critical value of 2.41. Above this

value the $B2$ structure becomes unstable. Therefore, one can imagine that the $B1$ phase in CaTe is not as stable as it is in the other compounds with smaller values of ionic radius ratio.

Regarding the indexing of the intermediate phase in CaTe , we are convinced of the assignment of the orthorhombic lattice because of very good agreement between the observed and calculated d spacings. Among many types of orthorhombic structures, the MnP structure best satisfies the constraints listed earlier. But we do not exclude other orthorhombic structures which could also be indexed to the intermediate phase. Angular dispersive x-ray-diffraction techniques may be helpful in further confirming the crystal structure of CaTe in the intermediate phase. We note that the MnP structure has the same space group and basis as that of the GeS structure (also orthorhombic). The difference between these two structures is the shape of the unit cell. The GeS structure has been assigned to the intermediate phase between the $B1$ and $B2$ phases in NaBr and NaI under high pressure.²⁹ It was the shape of the unit cell that made us favor the MnP structure over the GeS structure.

V. CONCLUSIONS

The present work on CaX ($X = \text{S, Se, Te}$) has completed the structural transformations in calcium chalcogenides from the sixfold-coordinated $B1$ structure to the eightfold-coordinated $B2$ structure. Only CaTe experiences an intermediate state possibly with a mixture of NaCl and MnP phases. The initial $B1$ structure in CaX becomes unstable at fractional volumes of 0.70–0.74 and the volume decreases at the transformation range from 4 to 10 %. Both the transition pressures and bulk moduli follow the same general trends with the ionic radii similar to that found in other alkaline-earth chalcogenides. All the structural phase transition processes found in compression are reversible in decompression, including the intermediate phase in CaTe .

ACKNOWLEDGMENTS

We acknowledge the support by the Cornell Materials Science Center through the National Science Foundation under Grant No. DMR 91-21654 and by the National Science Foundation under Grant No. DMR 92-18249. We thank the CHESS staff for their technical assistance.

- ¹A. L. Ruoff, in *Materials Science and Technology*, edited by R. W. Cahn, P. Haasen, and E. J. Kramer (VCH, New York, 1991), Chap. 8, Vol. 5.
- ²L. Liu, *J. Appl. Phys.* **42**, 3702 (1971).
- ³L. Liu and W. A. Bassett, *J. Geophys. Res.* **77**, 4934 (1972).
- ⁴S. T. Weir, Y. K. Vohra, and A. L. Ruoff, *Phys. Rev. B* **33**, 4221 (1986).
- ⁵R. Jeanloz, T. Ahrens, H. K. Mao, and P. M. Bell, *Science* **206**, 829 (1979).
- ⁶J. F. Mammone, H. K. Mao, and P. M. Bell, *Geophys. Res. Lett.* **8**, 140 (1981).
- ⁷P. Pichet, H. K. Mao, and P. M. Bell, *J. Geophys. Res.* **93**, 15 279 (1988).
- ⁸H. G. Zimmer, H. Winzen, and K. Syassen, *Phys. Rev. B* **32**, 4066 (1985).
- ⁹M. Baublitz, Jr., V. Arnold, and A. L. Ruoff, *Rev. Sci. Instrum.* **52**, 1616 (1981).
- ¹⁰K. E. Brister, Y. K. Vohra, and A. L. Ruoff, *Rev. Sci. Instrum.* **57**, 2560 (1986).
- ¹¹J. C. Jamieson, J. Fritz, and M. H. Manghnani, *Adv. Earth Planet. Sci.* **12**, 27 (1980).
- ¹²F. Birch, *J. Geophys. Res.* **83**, 1257 (1978).
- ¹³T. L. Huang and A. L. Ruoff, *Phys. Rev. B* **27**, 7811 (1983).
- ¹⁴A. Werner, H. D. Hochheimer, K. Strossnet, and A. Jayaraman, *Phys. Rev. B* **28**, 3330 (1983).
- ¹⁵T. L. Huang and A. L. Ruoff, *Phys. Rev. B* **31**, 5976 (1985).
- ¹⁶T. Chatteropadhyay, H. G. Von Schnering, W. A. Grosshans, and W. B. Holzapfel, *Physica* **139&140B**, 356 (1986).
- ¹⁷R. W. G. Wyckoff, *Crystal Structures* (Interscience, New York, 1971), Vol. 1, p. 102.
- ¹⁸T. Kamimura, M. Sato, H. Takahashi, N. Mori, H. Yoshida, and T. Kaneko, *J. Magn. Magn. Mater.* **104-107**, 255 (1992).
- ¹⁹R. D. Shannon, *Acta Crystallogr. A* **32**, 751 (1976).
- ²⁰K. Syassen, *Physica* **139&140B**, 277 (1986).
- ²¹H. Luo, R. G. Greene, and A. L. Ruoff, *Phys. Rev. B* **49**, 15 341 (1994).
- ²²Y. K. Vohra, S. J. Duclos, and A. L. Ruoff, *Phys. Rev. Lett.* **54**, 570 (1985).
- ²³T. L. Huang and A. L. Ruoff, *Phys. Rev. B* **29**, 1112 (1984).
- ²⁴K. Asaumi, *Phys. Rev. B* **29**, 1118 (1984).
- ²⁵E. Knittle and R. Jeanloz, *Science* **223**, 53 (1984).
- ²⁶T. L. Huang, K. E. Brister, and A. L. Ruoff, *Phys. Rev. B* **30**, 2968 (1984).
- ²⁷E. Knittle, A. Ruby, and R. Jeanloz, *Phys. Rev. B* **30**, 588 (1985).
- ²⁸K. Ghandehari, H. Luo, A. L. Ruoff, S. S. Trail, and F. J. DiSalvo (unpublished).
- ²⁹T. Yagi, T. Suzuki, and A. Akimoto, *J. Phys. Chem. Solids* **44**, 135 (1983).